Protein Science (1993), *2*, 739-752. Cambridge University Press. Printed in the USA.

Crystal structure analysis of amicyanin and apoamicyanin from *Paracoccus denitrificans* at 2.0 Å and 1.8 Å resolution

ROSEMARY DURLEY,[1] LONGYIN CHEN,[1] LOUIS W. LIM,[2]
F. SCOTT MATHEWS,[1] AND VICTOR L. DAVIDSON[3]

[1] Department of Biochemistry and Molecular Biophysics,
Washington University School of Medicine, St. Louis, Missouri 63110
[2] Department of Chemistry, Southern Illinois University, Carbondale, Illinois 62901
[3] Department of Biochemistry, University of Mississippi Medical Center,
Jackson, Mississippi 39216

(RECEIVED October 20, 1992; REVISED MANUSCRIPT RECEIVED January 21, 1993)

Abstract

The crystal structure of amicyanin, a cupredoxin isolated from *Paracoccus denitrificans*, has been determined by molecular replacement. The structure has been refined at 2.0 Å resolution using energy-restrained least-squares procedures to a crystallographic residual of 15.7%. The copper-free protein, apoamicyanin, has also been refined to 1.8 Å resolution with residual 15.5%.

The protein is found to have a β-sandwich topology with nine β-strands forming two mixed β-sheets. The secondary structure is very similar to that observed in the other classes of cupredoxins, such as plastocyanin and azurin. Amicyanin has approximately 20 residues at the N-terminus that have no equivalents in the other proteins; a portion of these residues forms the first β-strand of the structure.

The copper atom is located in a pocket between the β-sheets and is found to have four coordinating ligands: two histidine nitrogens, one cysteine sulfur, and, at a longer distance, one methionine sulfur. The geometry of the copper coordination is very similar to that in the plant plastocyanins. Three of the four copper ligands are located in the loop between β-strands eight and nine. This loop is shorter than that in the other cupredoxins, having only two residues each between the cysteine and histidine and the histidine and methionine ligands. The amicyanin and apoamicyanin structures are very similar; in particular, there is little difference in the positions of the coordinating ligands with or without copper.

One of the copper ligands, a histidine, lies close to the protein surface and is surrounded on that surface by seven hydrophobic residues. This hydrophobic patch is thought to be important as an electron transfer site.

Keywords: amicyanin; electron transfer; methylamine dehydrogenase; *Paracoccus denitrificans*; type I blue copper protein

Amicyanins are one class of type I copper proteins (cupredoxins; Adman, 1985), which contain a single copper site and transfer a single electron along an electron transfer pathway. Several excellent reviews have covered the type I proteins, notably by Ryden (1984), Adman (1985), and Chapman (1991). The amicyanins play a critical role in the respiratory chains of certain methylotrophic bacteria. Their primary role appears to be acceptance of an electron from methylamine dehydrogenase (MADH) and transfer of an electron to one or more *c*-type cytochromes. Amicyanin was first isolated from *Methylobacterium extorquens* AM1 (then known as *Pseudomonas* AM1), grown on methylamine (Tobari & Harada, 1981). It has subsequently been isolated from other bacteria grown on methylamine (Husain & Davidson, 1985). The amino acid sequences of amicyanin from three bacteria, *M. extorquens* AM1 (Ambler & Tobari, 1985), *Thiobacillus versutus* (van Beeumen et al., 1991), and *Paracoccus denitrificans* (van Spanning et al., 1990), have been determined and are shown in Figure 1.

Several classes of cupredoxins, namely, azurin, plastocyanin, pseudoazurin, and cucumber basic protein, have

Reprint requests to: F. Scott Mathews, Department of Biochemistry and Molecular Biophysics, Washington University School of Medicine, 660 S. Euclid Ave., Box 8231, St. Louis, Missouri 63110.

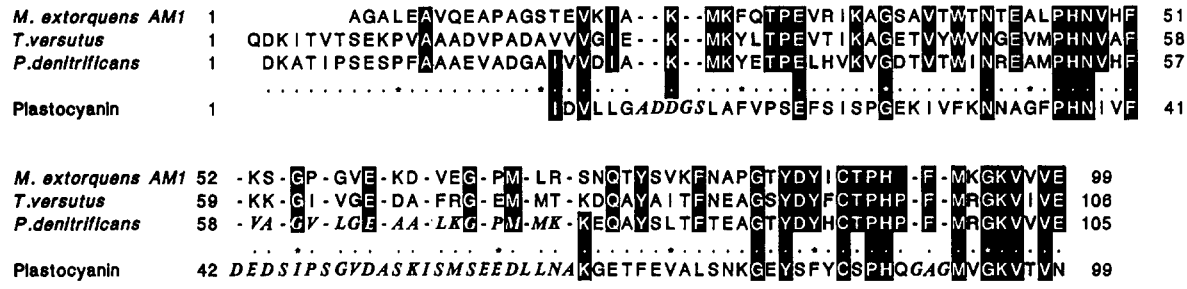

Fig. 1. The sequences of amicyanin from *Methylobacterium extorquens* AM1, *Thiobacillus versutus*, and *Paracoccus denitrificans* aligned to the sequence of poplar plastocyanin (Guss & Freeman, 1983). The alignment with plastocyanin is based on comparisons of the backbone structures. Three segments in the plastocyanin structure—7–11, 42–65, and 89–91—corresponding to position 27, segment 58–73, and position 97 in the amicyanin structure, were omitted from the alignment along with the first 20 residues of amicyanin. All of the omitted residues are shown in italics. Mismatched segments were identified where the equivalent C_α atoms deviated by more than 2.0 Å. The running sequence numbering refers to the *P. denitrificans* sequence with an asterisk representing every 10th residue. The boxed residues indicate sequence identities either for poplar plastocyanin with *P. denitrificans* amicyanin, for the three amicyanin sequences, or for all four sequences together.

now been studied by X-ray crystallography. Two of these, plastocyanin and azurin, have been investigated most extensively. High-resolution structures (2.0 Å or better) of plastocyanin from poplar (Guss & Freeman, 1983) and from *Enteromorpha prolifera* (Collyer et al., 1990) and of azurin from *Alcaligenes denitrificans* (Baker, 1988) and from *Pseudomonas aeruginosa* (Nar et al., 1991) have been reported. Furthermore, high-resolution crystallography has been used to study the plastocyanin structure over a considerable range of pH (Guss et al., 1986), as well as the structures of apoplastocyanin (Garrett et al., 1984) and apoazurin (Nar et al., 1992). The structure of pseudoazurin from *Alcaligenes faecalis* S-6 has been determined at 1.55 Å resolution (Petratos et al., 1988) and of the cucumber basic protein at 3.0 Å resolution (Guss et al., 1988). These studies have led to the conclusion that the folding of the polypeptide chain imposes a characteristic geometry on the type I copper site. The copper coordination of plastocyanin, pseudoazurin, and cucumber basic protein can be described as distorted tetrahedral with two histidine ligands binding through the N^δ of the imidazole ring, one cysteine ligand binding through its sulfur atom, and one methionine ligand, also binding through its sulfur atom, but at a longer distance. The copper coordination in azurin includes a fifth ligand formed by the main-chain carbonyl oxygen atom, which precedes the first sequential histidine ligand.

The amicyanins have been found to comprise a distinct subclass of cupredoxins. This class has absorption and electron paramagnetic resonance spectra characteristic of the type I copper proteins (Husain & Davidson, 1985), and resonance Raman studies (Sharma et al., 1988) indicate a copper coordination, which is similar to, but distinct from, plastocyanin. A further similarity to the plastocyanins is observed in the lability of the copper site at low pH, where one of the histidines of reduced plastocyanin becomes protonated, causing dissociation from the copper with resultant loss of redox activity. Sequence comparisons also suggest similarity to the plastocyanins based on the alignment of putative copper ligands (van Beeumen et al., 1991), even though there is little sequence homology (approximately 20% identity). Furthermore, the alignment indicates that the amicyanins are approximately 20 residues longer at the amino-terminal end. In addition, the loop containing three of the four copper ligands in amicyanin is somewhat shorter, as compared to the plastocyanins of green plants and the azurins of bacteria.

We present herein the X-ray crystal structure determination of an amicyanin, isolated from *P. denitrificans* (Husain & Davidson, 1985) and crystallized by Lim et al. (1986). This protein contains 105 amino acid residues of known sequence (Fig. 1) plus a single copper atom for a total molecular mass of 11.6 kDa. It is hoped that investigation of the amicyanin structure will help further our understanding of this characteristic copper environment and how the amicyanins transfer electrons from MADH to their cytochrome partners.

Results and discussion

Overall description of the molecule

The Ramachandran diagrams (Ramachandran & Sasisekharan, 1968) for both amicyanin and apoamicyanin are shown in Figure 2A and B, respectively. Three of the residues have conformational angles in the left-handed 3_{10}-helical region. A high β-sheet content is reflected in the Ramachandran plot where the majority of (ϕ, ψ) angles are clustered around $(-120°, +135°)$. The temperature factors for the main-chain and side-chain atoms of each protein, averaged over the individual atoms of each residue, are shown in Figure 3A and B. The region of the structure with the highest B values (residues 15–20) corresponds to a loop with weak electron density. This por-

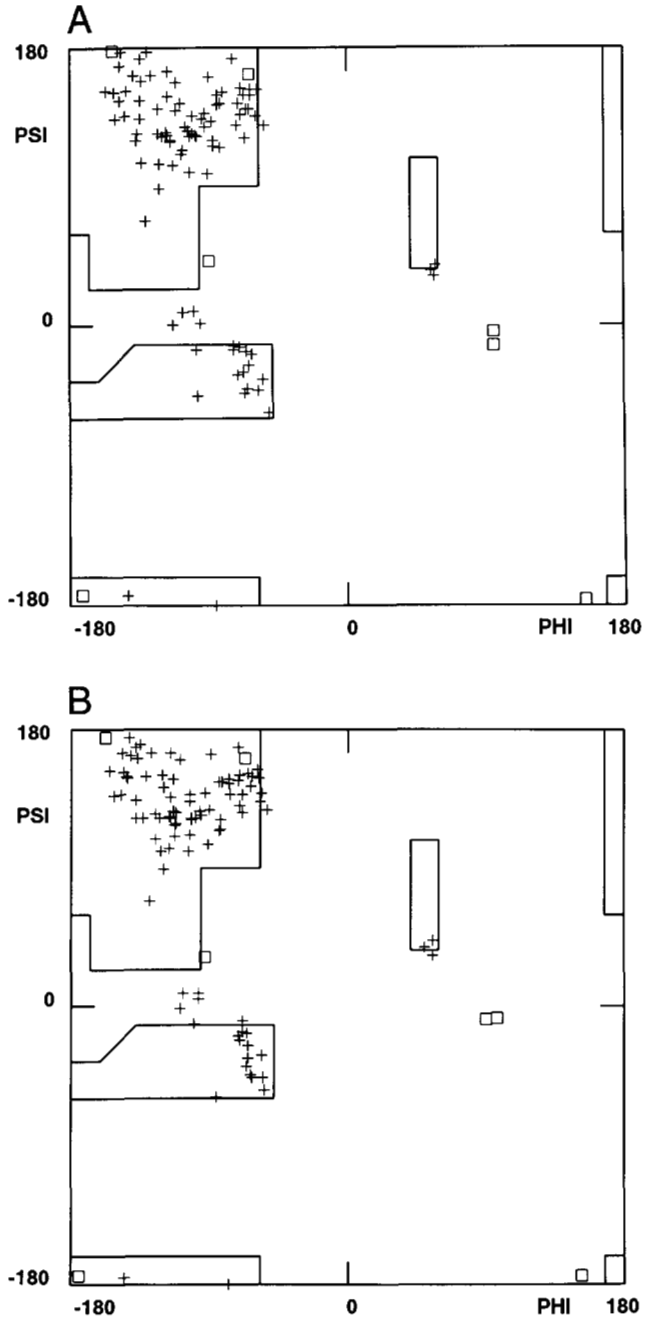

Fig. 2. Ramachandran diagram for amicyanin (**A**) and for apoamicyanin (**B**). Glycine residues are represented by squares, and all other amino acids are represented by crosses.

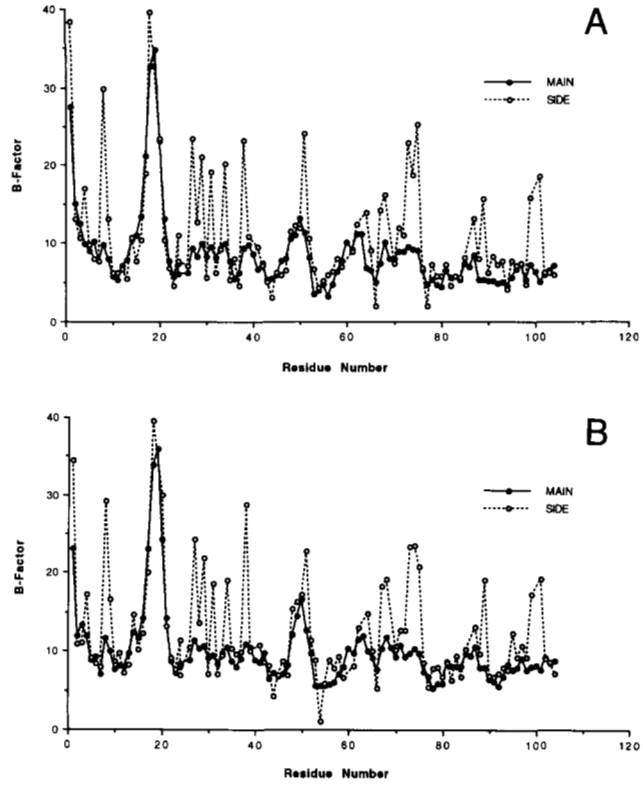

Fig. 3. The temperature factors, in $Å^2$, plotted against residue number. The average of the temperature factors for main-chain atoms of each residue is shown with filled circles, and the average of the temperature factors for the side chain of each residue is shown with open circles. **A:** Amicyanin. **B:** Apoamicyanin.

tion of the structure is not involved in any β-sheets and is not stabilized by ordered solvent.

The topology of the amicyanin backbone is shown in Figure 4A. Figure 5 and Kinemage 1 show the C_α structure with the copper ligands included. Amicyanin consists of nine β-strands that form a β-sandwich structure. The protein topology is very similar to that of plastocyanin, azurin, and pseudoazurin. However, the extended N-terminal portion of amicyanin forms an irregular outer β-strand, strand 1, which is not present in the other cupredoxins that have been studied so far. Strands 1, 7, 4, 2, 3 form a mixed sheet A, and strands 3′, 9, 8, 5, 6 form the mixed sheet B. There are no helical regions in amicyanin. The copper atom is situated in a pocket between the two sheets at one end of the molecule (often called the "northern" end, at the top of Fig. 5). The interior of the β-sandwich is lined with hydrophobic groups and is rich with aromatic residues. There are several polar residues in the interior. Two of these, Tyr^{78} and Tyr^{90}, which are conserved in the amicyanins (Fig. 1; Kinemage 2), flank Trp^{45}, located in the center of the molecule, with Tyr^{90} forming a hydrogen bond to N^{ϵ} of the tryptophan.

The copper site of amicyanin, illustrated in Figure 6, primarily has N_2S coordination at relatively close distances with a fourth sulfur ligand at a longer distance. These findings are in agreement with results obtained by Raman spectroscopy (Sharma et al., 1988) and extended X-ray absorption fine structure (EXAFS) spectroscopy (Lommen et al., 1991a). One close ligand, His^{53} $N^{\delta 1}$, is found at the beginning of strand 5, and the other two close ligands, Cys^{92} S^{γ} and His^{95} $N^{\delta 1}$, are found between

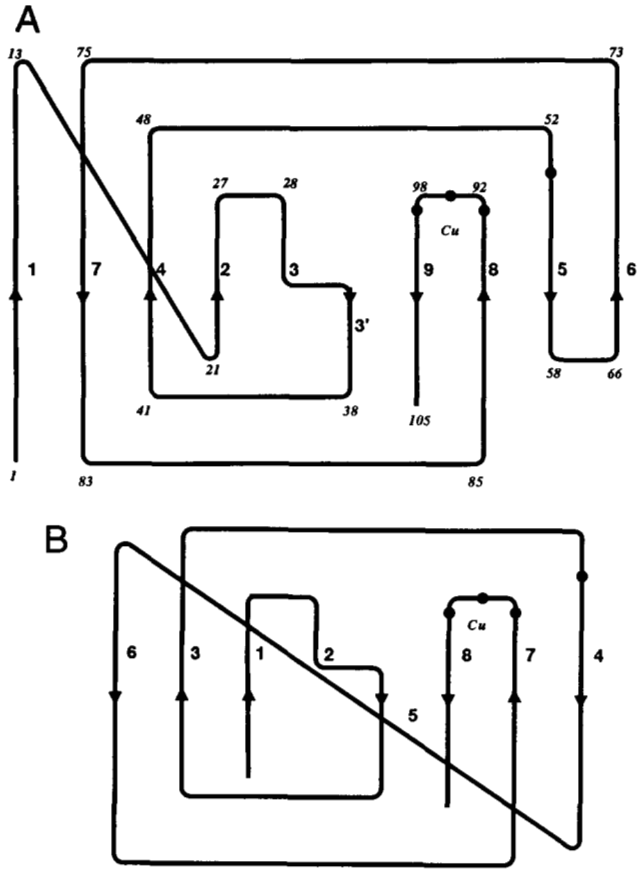

Fig. 4. Schematic folding pattern and numbering scheme for the β-strands of amicyanin (**A**) and for plastocyanin (**B**). The numbering scheme for plastocyanin is taken from Guss and Freeman (1983; reproduced with modification with permission from *Nature*).

strands 8 and 9. The fourth (more distant) ligand, Met^{98} S^{δ}, is also found on this loop. The geometry of coordination may be described as distorted trigonal pyramidal or distorted tetrahedral. The bond lengths and angles are given in Table 1.

Table 1. *Copper site geometry*

Cu-ligand bond lengths (Å)	
Cu-ND1(53)	1.95
Cu-SG(92)	2.15
Cu-ND1(95)	2.00
Cu-SD(98)	2.89
Ligand-Cu-ligand bond angles (°)	
ND1(53)-Cu-SG(92)	135
ND1(53)-Cu-ND1(95)	109
ND1(53)-Cu-SD(98)	83
SG(92)-Cu-ND1(95)	109
SG(92)-Cu-SD(98)	109
ND1(95)-Cu-SD(98)	104
Deviations from plane through ND1(53), SG(92), ND1(95) (Å)	
Cu	0.30
SD(98)	3.08

Secondary structure

The secondary structure of amicyanin and apoamicyanin is dominated by nine β-strands that form two β-sheets. The β-strands and turns are summarized in Table 2, and the main-chain hydrogen-bonding pattern of the β-sheets is illustrated in Figure 7 and Kinemage 2. The procedure of Kabsch and Sander (1983) was used to identify the β-strands and turns. One additional turn, 92–95, was identified by inspection of the model. The first β-strand lies on one edge of β-sheet A but loops away from the sheet between residues 5 and 10. The third β-strand, on the other edge, is shared between the two sheets and has a kink where the hydrogen bonding shifts from sheet A to sheet B. Residue 32, at this kink, is a conserved threonine (Fig. 1; Kinemage 2). Both β-sheets have mixed parallel and antiparallel strands. Most main-chain C=O and NH groups are hydrogen bonded to other strands. All internal polar side chains are also involved in hydrogen bonds. Of these, Ser^{79} and Tyr^{30} are hydrogen bonded to surface and buried water molecules, respectively.

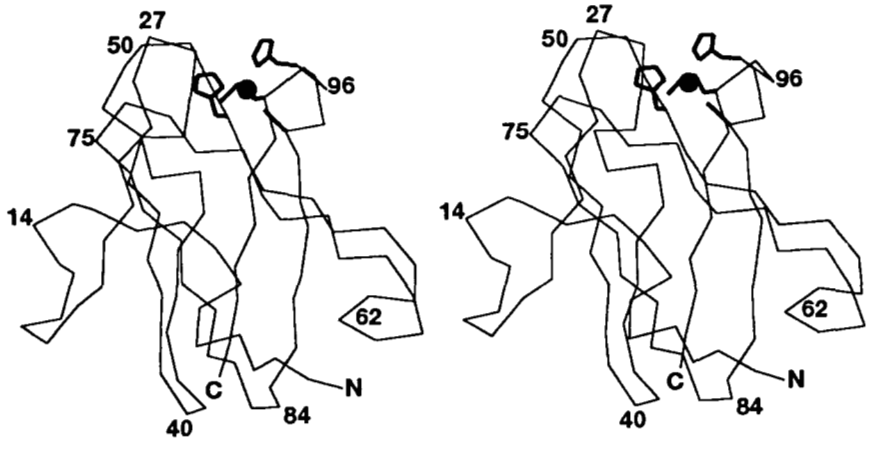

Fig. 5. Stereo diagram of the C_{α} backbone of amicyanin. The copper atom and four copper ligand side chains are included. The molecule forms a β-sandwich with two mixed β-sheets facing each other. The copper is located between the two sheets toward the top of the molecule, often referred to as the northern end. Several of the residues are numbered to help in following the polypeptide chain.

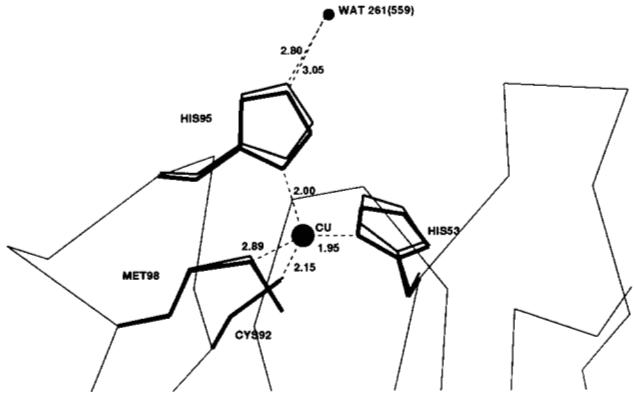

Fig. 6. The copper-binding site of amicyanin showing the bond distances (in Å) for the N_2S_2 coordination. Side chains shown in thick lines are for amicyanin and those in thin lines are for apoamicyanin. Also shown is the solvent molecule that forms a hydrogen bond to the N^{ϵ} atom of His^{95}, in both the amicyanin and the apoamicyanin structure.

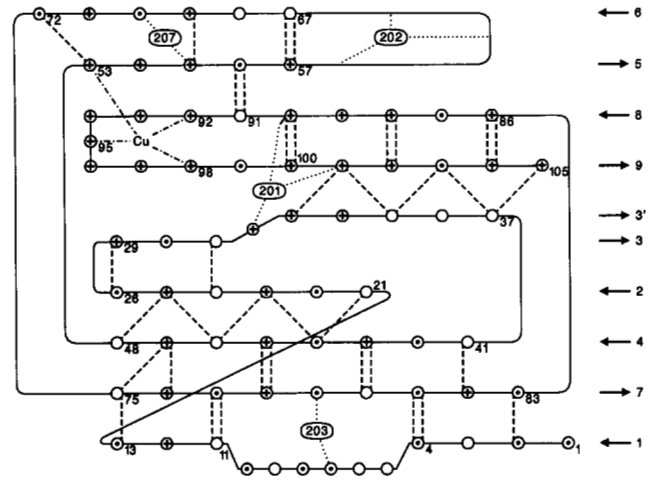

Fig. 7. The hydrogen-bonding pattern of the β-sheet structure of amicyanin. Hydrogen bonds are represented by dashed lines, with bonds from NH appearing on the N-terminal side of the residue while bonds to O appear toward the C-terminus. Residues that are invariant among all three amicyanins of known sequence are marked with a ⊕, while those that are conserved in two of the three are marked with a ⊙. All four internal waters have been included in this figure with their hydrogen bonds represented by dotted lines. The copper coordination is also shown.

The seven β-turns are listed in Table 2. Located within the turns are the three non-glycine residues (27, 28, and 75) with conformational angles near $\phi = +60°$, $\psi = +35°$, in the left-handed 3_{10} region of the Ramachandran diagram (Fig. 2). Lys^{27} and Met^{28} are involved in a type III′ turn, and Glu^{75} is involved in a type II turn. Type III′ and type II turns normally contain Gly at the second or third position of the turn in order to minimize steric repulsion. However, many exceptions to these generalizations occur (Chou & Fasman, 1977). For example, the turn at 73–76, consisting of Lys^{73}, Lys^{74}, Glu^{75}, and Gln^{76}, is associated with clear electron density (Fig. 8), and its geometry looks remarkably unhindered. The backbone N of Glu^{75} hydrogen bonds to Asn^{47}, which is conserved in all three amicyanins. The O of Glu^{75} is hydrogen bonded to the main-chain N of Ala^{13}. These bonds may help to further stabilize the turn.

Table 2. *Secondary structure of both amicyanin and apoamicyanin*

β-Strand	No.	Sheet	Turns	Type[a]
2–13	1	A	17–20	III
21–26	2	A	26–29	III′
29–31	3	A	38–41	II
33–37	3′	B	58–61	II
41–48	4	A	73–76	II
53–57	5	B	92–95[b]	I
67–72	6	B	95–98	I
75–83	7	A		
86–91	8	B		
100–105	9	B		

[a] Classified according to Venkatachalam (1968) and Crawford et al. (1973), based on the (ϕ, ψ) conformational angles.

[b] This turn is of the "near reverse turn" type (Crawford et al., 1973) because the n to $n + 3$ hydrogen bond has poor angular geometry.

The geometry of the seven-residue loop containing three of the four copper ligands in amicyanin, 92–98, has been of special interest since in all other cupredoxins this loop is two to four residues longer (Chapman, 1991). The amino acid sequence in this segment is identical in the three amicyanin sequences thus far determined (Fig. 1). This polypeptide loop, shown in Figure 9, contains two reverse turns in tandem (92–95 and 95–98), the ends of which contain the copper ligands. The 92–95 turn is a type I "near reverse turn" (Crawford et al., 1973) containing a weak hydrogen bond with poor angular geometry. The second reverse turn, 95–98, is a normal type I reverse turn with good hydrogen-bonding geometry. The efficient use of two tight turns separating the three copper ligands enables the copper coordination to be achieved with a minimum number of residues. Also shown in Figure 9, for comparison, are the copper-binding loops of azurin and plastocyanin. The four-residue turn linking Cys^{92} and His^{95} in amicyanin is nearly identical to that in plastocyanin (and in pseudoazurin) but is augmented to a six-residue turn in azurin, which extends further out into solution. On the other hand, the four-residue turn linking His^{95} and Met^{98} is shorter by one and two residues, respectively, than the corresponding loops in azurin and plastocyanin (and pseudoazurin).

The secondary structure of *T. versutus* amicyanin had been proposed from ^1H NMR experiments (Lommen

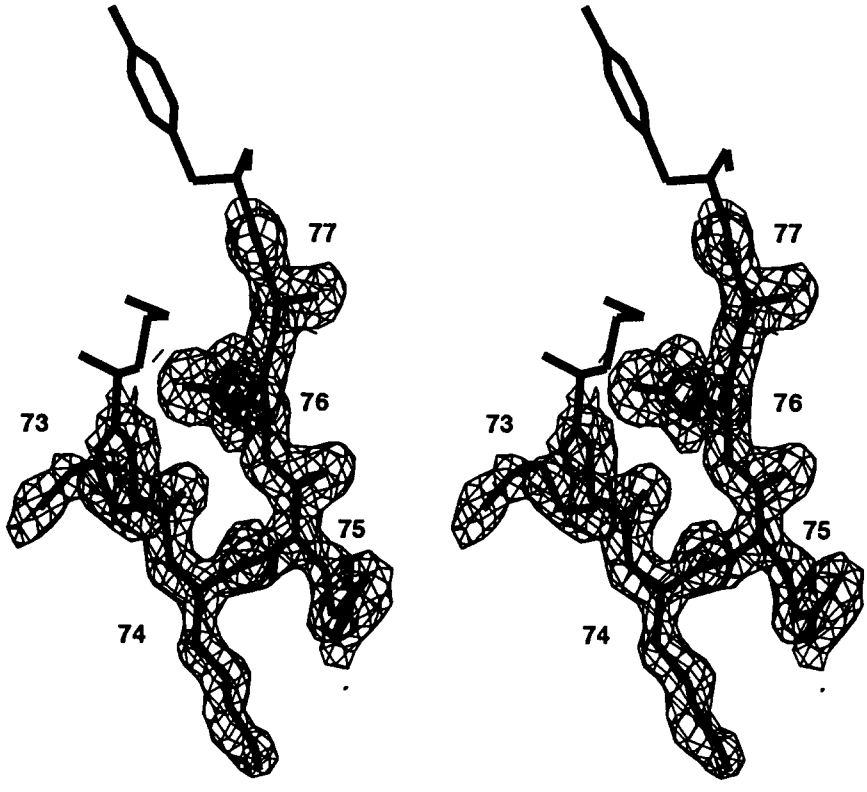

Fig. 8. Stereo diagram of the $2F_o - F_c$ map, contoured at 1σ, showing the region of the turn involving residues 73–76. This is a type II turn that would normally contain a Gly at the third position. In amicyanin this position is occupied by Glu^{75}.

et al., 1991b). Sequence comparisons with plastocyanin were used in assignment of the ^1H NMR spectrum. A secondary structure analysis was then performed. This study correctly identified the initial β-strand of amicyanin, which forms a part of sheet A and has no equivalence in the plastocyanin structure. The hydrogen-bonding patterns identified in this study are confirmed in the X-ray analysis. Only the hydrogen bonding between β-strands 5 and 6 had not been observed in the NMR studies. However, as noted below, this part of the crystal structure is stabilized by two solvent molecules and may be more mobile in solution.

Side-chain to main-chain hydrogen bonding

Table 3 lists the side-chain to main-chain hydrogen bonds for amicyanin and apoamicyanin. There are 12 side chains involved in these interactions. Six of these are conserved in all three amicyanin sequences, whereas only two are unique to the *Paracoccus* amicyanin. This level of conservation illustrates the importance of this type of interaction in stabilizing the structure. Of these 12 side chains, five are internal and the other seven are surface residues. Of particular interest are bonds where the side-chain and main-chain atoms link sequentially different parts of the

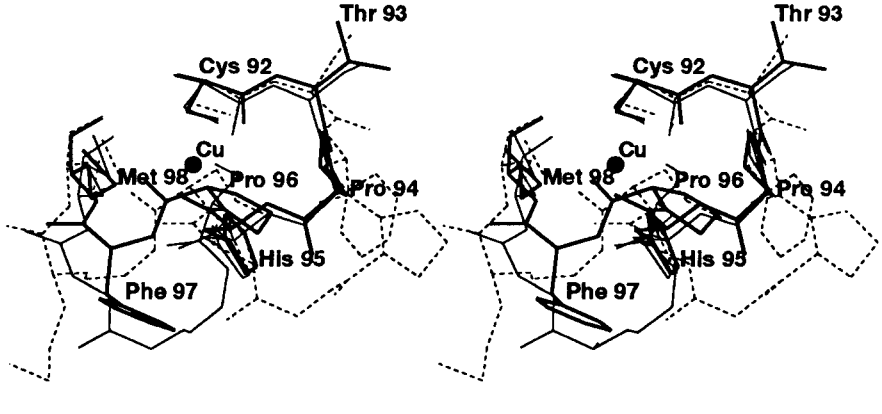

Fig. 9. Stereo diagram of the copper atom and the copper-binding loop of amicyanin (heavy lines) compared with those of plastocyanin (light lines) and azurin (dashed lines) superimposed. The seven residues, which are identified for amicyanin, form two reverse turns in tandem. For the first loop, 92–95, the plastocyanin backbone is identical in length and nearly congruent to amicyanin, while azurin contains two additional residues. The second loop, 95–98, is longer in both plastocyanin and azurin, by one and two residues, respectively.

Table 3. *Side-chain–main-chain hydrogen bonds*[a]

Atom 1	Atom 2	Distance (Å)	
		Amicyanin	Apoamicyanin
Glu[15] OE2	Ala[12] N	3.03	3.02
Tyr[30] OH	Asn[54] O	2.83	2.77
Asp[41] OD2	Lys[38] N	2.99	2.96
Asn[47][b] OD1	Met[51] O	3.03	3.09
Asn[47] OD1	Met[72] O	3.01	3.01
Glu[49] OE1	Lys[27] N	3.10	3.09
Glu[49] OE2	Met[28] N	2.92	2.96
Asn[54] ND2	Gly[69] O	3.00	2.97
Asn[54] OD1	Thr[93] N	2.85	2.83
Lys[74] NZ	Arg[48] O	3.10	3.36
Gln[76] OE1	Lys[73] N	3.19	3.07
Thr[83] OG1	Lys[2] O	3.26	3.07
Tyr[88] OH	Glu[84] O	2.80	2.88
Cys[92] SG	Asn[54] N	3.66	3.61
Arg[99] NE	Pro[96] O	2.73	2.79

[a] A distance cut-off of 3.25 Å for N to O or O to O hydrogen bonds was used for each protein. However, if a hydrogen bond was observed in one model, then the equivalent distance is given for the other protein.

[b] Invariant residues for *Paracoccus denitrificans*, *Thiobacillus versutus*, and *Methylobacterium extorquens* AM1 amicyanin are underlined.

Table 4. *Side-chain–side-chain hydrogen bonds*

Atom 1	Atom 2	Distance (Å)	
		Amicyanin	Apoamicyanin
Asp[24] OD2	Arg[48] NE	2.86	2.85
Asp[24] OD2	Arg[48] NH2	3.21	3.14
His[36] ND1	Glu[105][a] OE1	3.04	3.03
Thr[42] OG1	Thr[81] OG1	2.92	2.79
Thr[44] OG1	Ser[79] OG	2.85	2.77
Trp[45] NE1	Tyr[90] OH	3.04	3.05
Arg[48] OD2	Glu[75] OE1	3.16	2.75
Glu[49] OE2	His[53] NE2	2.71	2.75
Asn[54] ND2	Thr[93] OG1	2.93	2.90
His[56] ND1	Thr[93] OG1	2.71	2.74

[a] Underlined residues are invariant in the three sequenced amicyanins in Figure 1.

polypeptide chain. Seven side chains are involved in such bonds. Four of these are conserved in all three amicyanin sequences while the other three are conserved in two of the sequences. The most important such hydrogen bond is between S^{γ} of Cys[92] and the NH of Asn[54] (Kinemage 1). This hydrogen bond had been predicted from the Raman spectrum (Sharma et al., 1988) and helps stabilize the orientation of the cysteine ligand. The side-chain oxygen atoms of conserved Glu[49] hydrogen bond with NH of residues 27 and 28. Asn[47] hydrogen bonds with carbonyl oxygens of residues 51 and 72, and Asn[54] binds with residues 69 and 93. The hydroxyl OH of Tyr[30] hydrogen bonds with the carbonyl O of residue 54. This Tyr is retained in *P. denitrificans* and *T. versutus* but has been replaced by a Phe in *M. extorquens* AM1. The Phe is aromatic and has a similar size to Tyr but would not have an available hydrogen to cross-link the structure. The two remaining partially conserved side chains linking distant parts of the molecule are Thr[83], which is linked to residue 2 near the N-terminus, and Lys[74], which binds to the carbonyl O of residue 48. Thr[83] is replaced by Asn in both the other species while Lys[74], conserved in *T. versutus*, is replaced by Ser in *M. extorquens* AM1.

Side-chain to side-chain hydrogen bonds

Of the 10 side-chain to side-chain hydrogen bonds listed in Table 4, three are formed by pairs of invariant residues. The bond from His[53] to the carboxyl oxygen of Glu[49] and the bonds from the N^{δ} atoms of Asn[54] and His[56] to the hydroxyl of Thr[93] are close to the copper-binding pocket, helping to link the A and B sheets and stabilize the metal site. These bond distances are very similar in the holo and apo proteins. The bond formed between the invariant residues Trp[45] and Tyr[90] is significant in that it also links the two β-sheets (Kinemage 2). Arg[48] of β-strand 4 forms bonds to side chains on two neighboring strands, Asp[24] on strand 2, and Glu[75] on strand 7. All the other interactions are between side chains on adjacent strands.

Features of the molecular surface

The copper site with the ligand His[95] exposed at the protein surface is shown in Figure 6. This portion of the molecular surface is of particular interest, as it maintains contact with the MADH molecule in the crystalline complex (Chen et al., 1992) and is thought to be a potential electron transfer site. Surrounding the His[95] of amicyanin are seven hydrophobic residues—Met[71], Met[51], Met[28], Pro[52], Pro[94], Pro[96], and Phe[97]—all of which form most of the interface in the complex (Kinemage 1). Six of these residues are conserved in all three amicyanins, while the seventh, Met[51], is conserved in *T. versutus* and conservatively replaced by Leu in AM1.

There are three other surface features of note. The lower end of the molecule is composed of three loops, between β-strands 3–4, 5–6, and 7–8, and contains both the N- and C-termini of the structure. The loops are rich in acidic groups and include three Glu and three Asp side chains that extend from the bottom surface to form an acidic cluster.

One side of the amicyanin is distinctive, having a line of four positively charged residues lying just below the level of the copper site. These four surface residues are His[91], His[56], Lys[68], and Arg[99]. The remainder of this face consists of nonpolar or hydrophobic residues.

The opposite face to that described above contains several polar residues. The upper part of the surface has a mixture of charged groups, while the mid plane is hydrophobic and the lower portion, like the upper part, has a number of polar groups.

Crystal packing

The crystal lattice of amicyanin is very tightly packed, with no solvent-filled channels between molecules apparent in the lattice. This is consistent with the relatively small fractional solvent content of the crystals, 32%.

The intermolecular hydrogen-bonding interactions for amicyanin and apoamicyanin are given in Table 5. There are a total of 10 discrete hydrogen bonds per molecule, involving 17 separate residues. Four of these hydrogen bonds are main-chain to side-chain interactions, two of which involve charged side chains. Of the remaining, four are salt bridges between oppositely charged side chains and two are interactions between acidic side chains. In order for the latter interactions to be true hydrogen bonds, at least one of the carboxylate oxygens in each of these pairs should be protonated.

The 17 residues are clustered into six groups, each of which interacts with one other molecule in the lattice so that each amicyanin molecule is in contact with six of its neighbors. The crystallographic symmetry precludes interaction between the copper ligands of any two molecules in the lattice.

The atoms in the β-turn from residue 17–20 have a much higher temperature factor than the other atoms in the amicyanin structure (Fig. 2). This loop is on the protein surface and extends into a solvent-filled region of the lattice. Interestingly, the residue at position 18, Asp, forms a salt bridge with Lys^{29} on another molecule. The linkage seems to be too weak, however, to immobilize the 17–20 loop.

Solvent structure

Eighty-nine water molecules were included in the amicyanin and 98 in the apoamicyanin models. Of the 89 water molecules included for amicyanin, 78 have an equivalent position in the apoamicyanin structure. The water molecules were initially identified by ranking their peak heights as observed in the $F_o - F_c$ electron density maps. Consequently, the numbering of the water molecules reflects their initial electron density. Between the two proteins the equivalent waters generally appear at similar levels of electron density. For the purposes of discussion the waters of amicyanin have been numbered from 201 while those of apoamicyanin have numbers starting with 501.

Several of the water molecules are situated in the interior of the protein (Figs. 7, 10). Water 201 forms three hydrogen bonds at distances of 2.77, 2.71, and 2.88 Å with O^{32}, $TyrOH^{90}$, and O^{101}, respectively, each of these atoms being located on a different β-strand. It is at residue 32 that β-strand 3 twists to form part of sheet B. Water 202 also forms three hydrogen bonds, at distances of 2.79, 2.76, and 2.98 Å with O^{58}, N^{62}, and O^{65}, respectively. This water appears to stabilize the loop containing residues 57–67. Water 203 forms four hydrogen bonds, at distances of 2.87, 2.73, 3.11, and 2.92 Å with N^7 and O^7, and N^{79} and O^{79}. Residue 7 is central to the segment in $\beta 1$, which loops out from the sheet while residue 79 lies in $\beta 7$. Also in the interior of amicyanin is found water 207 (506), which forms two hydrogen bonds, 3.20 and 2.82 Å to N^{55} and O^{70}, thus bridging β-strands 5 and 6.

The internal waters appear to play a crucial role in maintaining the tertiary structure of the protein (Fig. 7). In particular strand $\beta 6$ forms only three main-chain hydrogen bonds to $\beta 5$; however, two waters, 202 and 207 (503 and 506), bridge these strands and help to stabilize the loop containing residues 58–66. Water 201 seems to harness β-sheet B, whereas water 203 harnesses the irregular region of the first β-strand.

Another water of particular interest is 261 of amicyanin, which is hydrogen bonded at a distance of 3.05 Å with $N^{\epsilon 2}$ of His^{95}, the copper ligand (Fig. 6). In azurin a similarly bound water has been postulated to play a functional role in electron transfer (van de Kamp et al., 1991). The equivalent water in apoamicyanin, 559, also hydrogen bonds with $N^{\epsilon 2}$ of His^{95} at a distance 2.80 Å. It is noteworthy that His^{95} appears to be in the same orientation in apoamicyanin as in amicyanin, because the water molecule bound to the N^{ϵ} of this histidine is retained in both structures (waters 559 and 261, respectively). The difference in position between the waters of the two structures is 0.06 Å. This situation differs from that in plastocyanin where the analogous water is located differently in the holo and apo forms, indicating that the histidine ligand is in different orientations in the two forms (Garrett et al., 1984).

Table 5. *Intermolecular hydrogen bonds*

		Distance (Å)	
Atom 1	Atom 2	Amicyanin	Apoamicyanin
Lys^2 NZ	Glu^{15} OE1	2.82	2.78
Pro^6 O	Arg^{99} NH	2.97	3.15
Ser^9 OG	Ala^{85} N	2.99	3.12
Ala^{12} N	Glu^{84} OE2	3.04	3.11
Glu^{15} OE2	Glu^{84} OE1	2.62	2.70
Asp^{18} OD2	Lys^{29} NZ	3.13	3.26
Asp^{24} OD1	Lys^{68} NZ	3.18	2.98
Glu^{31} OE1	Lys^{68} NZ	2.90	2.90
Asp^{41} OD2	Glu^{64} OE2	2.67	2.66
Gln^{76} NE2	Thr^{83} O	2.99	3.02

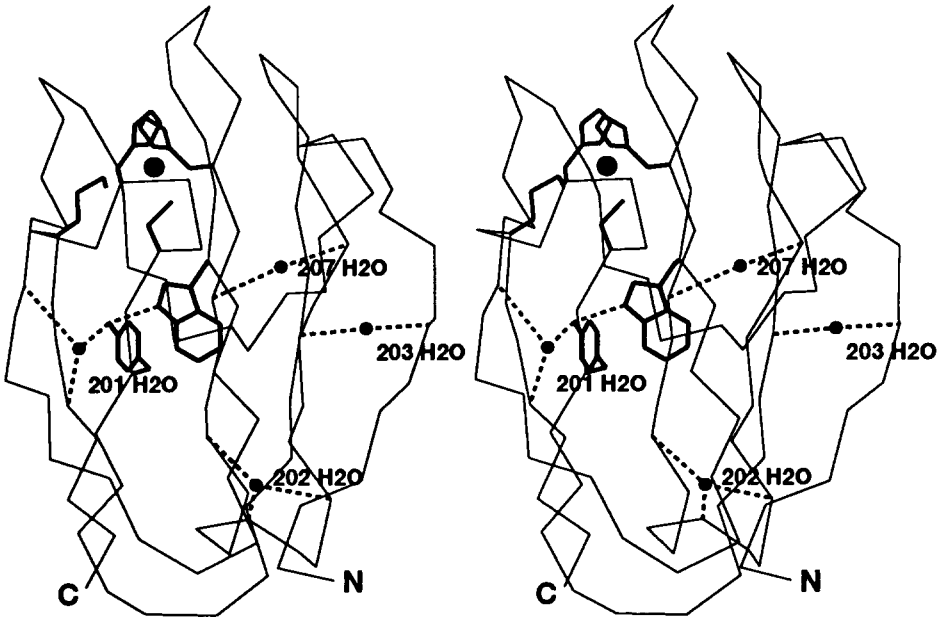

Fig. 10. Stereo diagram showing the four internal waters of amicyanin and their hydrogen-bonding interactions, which help to stabilize the tertiary structure of the molecule. The C_α chain is shown along with the side chains involved in the hydrogen bonding. The copper and copper ligands can also be seen at the top of the diagram.

Apoamicyanin structure

The removal of the copper atom from amicyanin seems to cause few structural changes, amounting to a difference in root mean square (rms) of 0.09 Å between C_α atoms. The copper site region (Fig. 6) shows few significant changes, although there appears to be a slight, but concerted, displacement of the copper ligand side chains, toward the protein surface.

Comparison to other cupredoxins

The topologies of the β-sheets are quite similar among the five classes of type I copper proteins. When all five structures are aligned, they have eight β-strands in common. Amicyanin has approximately 20 extra residues at the amino-terminal end, pseudoazurin has about 25 extra at the carboxy-terminal end, and azurin has about 30 residues inserted between strands 5 and 6 of the common barrel. Of the eight strands in common, the fifth strand differs most among the five families of copper proteins. The kink in strand 3 of amicyanin, which results in the first half being part of sheet A while the second half (3′) is part of sheet B, has been observed in all of the cupredoxins. Amicyanin is most similar in structure to plastocyanin and pseudoazurin, except for the N-terminal and C-terminal extensions described above. It differs to a greater extent from azurin and cucumber basic protein; a greater number of insertions and deletions is required to optimize structural alignment.

Examination of the copper-binding region of amicyanin, azurin, plastocyanin, and pseudoazurin reveals some interesting features. The hydrogen bond between the Cys^{92} ligand and the peptide NH of Asn^{54}, which stabilizes the orientation of the cysteine, is a conserved structural feature in all of these proteins and the identity of the asparagine is also conserved. The side-chain to side-chain hydrogen bond between Asn^{54} and Thr^{93} of amicyanin is also a conserved structural feature in these proteins except that the Asn is replaced by Ser in the azurins and one of the pseudoazurins contains Ala in place of Thr (Adman et al., 1989). On the other hand, the orientation of the first His ligand to copper (His^{53} in amicyanin) is stabilized by side-chain to side-chain interactions in amicyanin and pseudoazurin and by main-chain to side-chain interactions in azurin and plastocyanin.

The structural similarity between amicyanin and plastocyanin is striking (Fig. 11A). Generally the segments of polypeptide corresponding to β-strands 2, 3, 4, 5, 7, 8, and 9 of amicyanin (Fig. 4A) can be matched closely to the analogous segments of β-strands 1, 2, 3, 4, 6, 7, and 8 of plastocyanin (Fig. 4B). Specifically, 67 residues in four separate segments in each of the two proteins can be aligned with an rms difference between equivalent C_α atoms of 1.02 Å. When the aligned sequences of *P. denitrificans* amicyanin and poplar plastocyanin are compared (Fig. 1), 20 of the 67 residues (30%) are identical. Eighteen of these identities are maintained in all three amicyanins, four of which correspond to the copper ligands. The most significant nonmatched regions of amicyanin are segment 1–20, which has no counterpart in plastocyanin, segment 58–73 (approximately β6), which is in quite a different conformation from the corresponding segment 42–65 of plastocyanin (approximately β5), and position 97, where residues 89–91 of plastocyanin are inserted.

Amicyanin and pseudoazurin are also very similar in structure (Fig. 11B), even though the latter has 26 additional residues at the C-terminal end of the molecule.

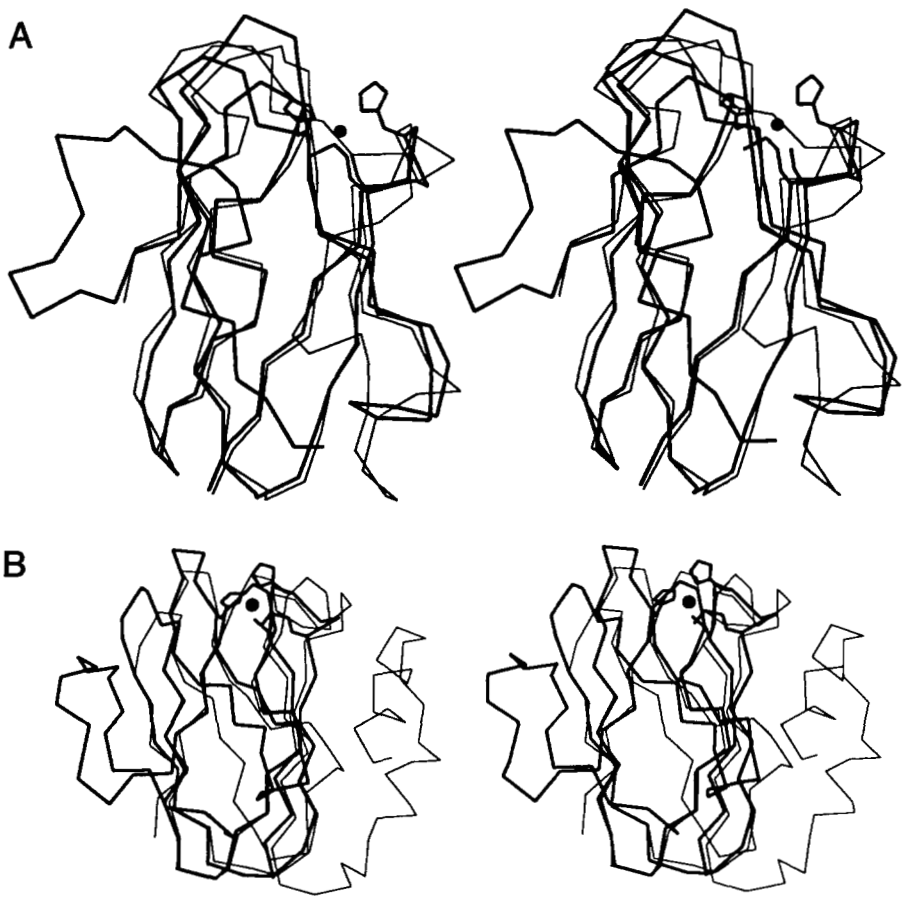

Fig. 11. Stereo diagrams of the C_α backbones of amicyanin (thick lines) superimposed on the poplar plastocyanin backbone (**A**) (thin lines) and the pseudoazurin backbone (**B**) (thin lines). The copper site for amicyanin is shown at the top of each diagram. The initial 20 residues of amicyanin, which, in part, form the large "loop" seen at the left of the two diagrams, have no counterpart in the plastocyanin nor pseudoazurin structures. Similarly, the last 26 residues of pseudoazurin, shown at the right in B, have no counterpart in amicyanin.

Alignment of 65 residues in the two proteins (Fig. 12), in six separate segments, yields an rms difference between equivalent C_α atoms of 0.84 Å and a sequence identity of 37% (24 out of 65). Fifteen of the 24 identities are maintained in all three amicyanin sequences. However, it is unclear whether or not amicyanin is significantly more similar to pseudoazurin than it is to plastocyanin given the greater segmentation of pseudoazurin required for alignment and the lower retention rate of sequence homology to it among the amicyanins.

The similarity of amicyanin to azurin is less pronounced. Alignment of the strands indicates that there are considerably more insertions and deletions in the two sequences and that the two structures show greater deviation than do the amicyanin–plastocyanin or amicyanin–pseudoazurin pairs. As with plastocyanin, strands 2–9 of amicyanin correspond approximately to strands 1–8 of azurin, but strand $\beta 5$ of azurin and its preceding turn differ from strand $\beta 6$ of amicyanin.

Based on the presence of a titratable histidine copper ligand and lack of disulfide bridges in amicyanin, it was postulated (van Beeumen et al., 1991) that amicyanin has a plastocyanin-type copper coordination rather than an azurin type. A comparison of their three-dimensional structures (Figs. 9, 11) confirms this hypothesis. However, the shorter loop between His^{95} and Met^{98} in amicyanin (Fig. 1) is clearly evident when its backbone conformation is compared to the longer loop in plastocyanin (Fig. 9). Despite this, the copper environments of the two proteins are practically superimposable. Like plastocyanin and unlike azurin the carbonyl oxygen of the residue preceding the first histidine ligand is too far from the copper (3.90 Å) to form a fifth ligand.

One of the most important surface features of amicyanin is the hydrophobic patch surrounding the exposed N^ϵ of the His^{95} ligand on the "northern" surface of the molecule. The conserved feature of an exposed histidine ligand surrounded by hydrophobic residues is considered of great importance as a potential electron transfer site. For amicyanin from *T. versutus* (Lommen & Canters, 1990) the titration and deuteration of His^{95} ($pK_a = 6.95$) had suggested a plastocyanin-like coordination of the copper, but the magnitude of the electron self-exchange rate and corresponding activation parameters suggested that the surface of amicyanin involved in electron transfer is more similar to azurin than to plastocyanin. In the amicyanin structure this patch contains seven residues, three Met, three Pro, and one Phe. The analogous hydrophobic surface patch in azurin consists of two Met, one Pro, one Phe, and one Gly surrounding the N^ϵ of the His 117,

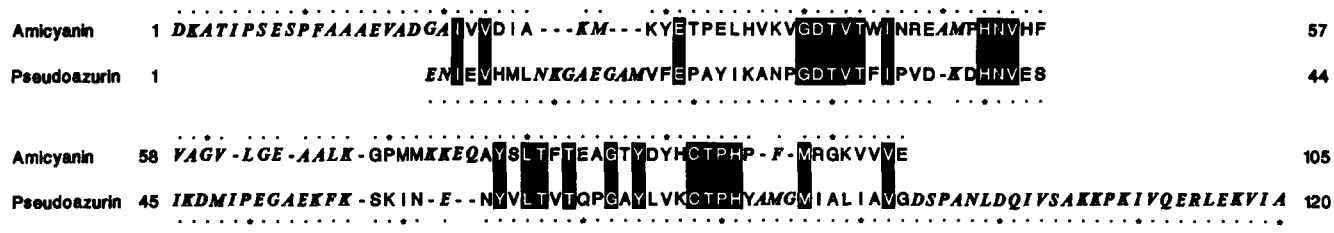

Fig. 12. The sequence of amicyanin from *Paracoccus denitrificans* aligned to the sequence of pseudoazurin from *Alcaligenes faecalis* S-6 (Petratos et al., 1988). The alignment with pseudoazurin is based on comparison of the backbone structures. Five segments in the pseudoazurin structure, 9–16, 38, 45–57, 62, and 83–85 corresponding to segments 27–28, 50–51, 58–68, 73–76, and 98 in the amicyanin structure, were omitted from the alignment along with the first 2 and the last 27 residues of pseudoazurin and the first 20 residues of amicyanin. All of the omitted residues are shown in italics. Mismatched segments were identified where the equivalent C_α atoms deviated by more than 2.0 Å. The upper running sequence numbering refers to amicyanin and the lower numbering to pseudoazurin, with * representing every 10th residue. The boxed residues indicate sequence identities between the two proteins.

which is coordinated to the copper. This ring of hydrophobic residues is conserved in all the azurins and is surrounded by a second concentric ring of surface hydrophobic residues beyond this patch. In the azurins this patch contributes many of the intermolecular interactions between the molecules in the crystal. Plastocyanin also has a hydrophobic north surface, although the corresponding patch is smaller than that observed in the azurins or in amicyanin. Notably, Phe^{97} of amicyanin has no counterpart in the hydrophobic surface of plastocyanin. This leaves the copper of plastocyanin more exposed to solvent than in azurin or amicyanin. However, the physical boundaries of the north surface of amicyanin are in fact more similar to those of plastocyanin since in azurin two loops (containing residues 39–44 and 114–117, which are equivalent to segments 50–52 and 94–95 of amicyanin) extend beyond the hydrophobic surface. The differences between these northern surfaces may be related to the receptor sites on their electron transfer partners. It has previously been noted that despite the similarities of structure, plastocyanin is a very poor electron acceptor for *P. denitrificans* MADH and does not form a complex with that protein (Gray et al., 1988).

A second "remote" electron transfer site has been studied extensively in the plastocyanins and azurins (He et al., 1991). The site consists of an acidic patch surrounding Tyr^{83} of plastocyanin. When the amicyanin and plastocyanin structures are superimposed, Tyr^{83} of plastocyanin is found to lie in a similar position to His^{91} of amicyanin. This histidine is not surrounded by acidic residues but rather lies next to a second histidine in the linear array of positively charged residues, His^{91}, His^{56}, Lys^{68}, and Arg^{99}, as described above. The two histidines are oriented in a similar manner to two of the histidine ligands of the type II copper site in ascorbate oxidase (Messerschmidt et al., 1992) and to two histidines of nitrite reductase (Godden et al., 1991). This line of positively charged residues runs along the surface just below the level of the copper-binding site. The remainder of this face consists of hydrophobic residues. The possibility of the histidine residues at this site acting as a second or alternate electron transfer site, in the amicyanin pathway, is somewhat diminished when it is noted that these histidines are not invariant or even maintained as aromatic residues in the other amicyanins.

Conclusions

The structure of a member of the amicyanin family of cupredoxins has now been solved. Although generally similar to other cupredoxins, amicyanin is most similar to plastocyanin and pseudoazurin, both in terms of the geometry of its copper coordination and its overall secondary structure. However, its structure is distinct from other cupredoxins in a number of ways, making the amicyanin family unique. First, there are approximately 20 residues at the N-terminal end that have no counterpart in the other well-characterized cupredoxins. Some of these form a new first β-strand of the β-sandwich. Second, the loop containing three of the four copper ligands, between the last two β-strands, is the shortest among the cupredoxins, with only two residues separating each of the ligands. This shortened loop creates the tightest geometry with minimal disruption of the coordination sphere. Third, the arrangement of surface residues on amicyanin is unique. The hydrophobic patch surrounding the exposed histidine ligand to copper is most similar to azurin, but differs substantially in detail. Other groupings of hydrophobic acidic or basic residues also differ from other cupredoxins and probably reflect the biological diversity among their redox partners.

Materials and methods

Crystallization

Amicyanin was prepared from cells of *P. denitrificans* grown with methylamine as the sole source of carbon

(Husain & Davidson, 1985). Apoamicyanin was prepared by extraction of the copper from the reduced protein by dialysis against KCN (Husain et al., 1986). Crystals of amicyanin and apoamicyanin were prepared by the macroseeding method as described previously (Lim et al., 1986). Prismatic crystals grow to 0.3–0.4 mm average dimension in 3.0 M (Na/K) phosphate solution, pH 6.5, from 1% protein solution under mineral oil. Seeds of approximately 0.05 mm dimension were used. For apoamicyanin, seeds of the holo protein were used, which represented less than 1% of the final crystal volume. The crystals of amicyanin and apoamicyanin are isomorphous, space group $P2_1$, with cell parameters $a = 28.90$ Å, $b = 56.61$ Å, $c = 27.55$ Å, and $\beta = 96.41°$. The crystals contain one molecule per asymmetric unit, have a solvent content of 32%, and diffract beyond 1.3 Å resolution.

Data collection

X-ray diffraction data from amicyanin and apoamicyanin were collected at 2.0 and 1.8 Å resolution, respectively, on a Picker 4-circle diffractometer as described previously (Lim et al., 1982). Friedel-related reflections were collected for the holo but not for the apo protein. A total of 6,030 reflections were recorded for amicyanin and 8,221 reflections for apoamicyanin. The overall crystal decay was approximately 18% for amicyanin and 14% for apoamicyanin. The data were corrected for Lorentz and polarization effects, radiation damage, and absorption effects as described previously. The apoamicyanin data were then locally scaled to the amicyanin data (Matthews & Czerwinski, 1975).

Structure analysis

Location of the copper position

A difference Patterson function was calculated at 2.5 Å resolution, using the holo minus the apoamicyanin structure factors as coefficients (see Table 6). The highest peak on the Harker section was observed at greater than nine times the background and was more than five times the magnitude of the next highest peak. This peak was located on the $v = \frac{1}{2}$ Harker section and was interpreted as the vector between the two copper atoms in the unit cell of the holo protein. It thus defined the copper position.

Table 6. *Isomorphous difference Patterson peaks*

u	*v*	*w*	Peak rank	% Maximum peak height
0.06	0.5	0.23	1	100
0.12	0.5	0.48	2	18

Single isomorphous replacement phases calculated from the copper position gave a highly ambiguous, centrosymmetric map, which could not be interpreted. Attempts to prepare heavy atom derivatives were unsuccessful.

Molecular replacement solution

Because plastocyanin and amicyanin were known to have some degree of sequence homology (van Beeumen et al., 1991), particularly in the copper-binding and β-sheet regions of the structure, molecular replacement methods (Crowther & Blow, 1967) were attempted using the program suite MERLOT (Fitzgerald, 1988). Initially the full model for the poplar plastocyanin, based on the 1.6-Å resolution model (Guss & Freeman, 1983), was used as a search probe. Later the plastocyanin search model was stripped down to include only the β-sheet structure, and later still, only the main chain and conserved side chains. None of these search probes produced a consistent rotation function solution. The resolution range of the data and Patterson search radius were also varied, but to no avail.

Meanwhile, a binary complex of MADH and amicyanin had been crystallized (Chen et al., 1988). This structure was solved by molecular replacement using native MADH from *T. versutus* as the search probe, and the amicyanin molecule was subsequently traced (Chen et al., 1992). The amicyanin structure from the complex was then used as a search probe in the present study. Only one resolution range was used, 4–8 Å, with a Patterson search radius of 20 Å. The search model was initially translated in order to place the copper atom at the origin. This meant that the translation function solution should equate to the copper vector already observed in the amicyanin difference map. Table 7 shows the results of molecular replacement. The highest rotation peaks show the clear superiority of one rotation vector. The translation search was performed after rotation by the Euler angles from peak 1 of the rotation search. Application of the three Euler angles and the translation vector to the starting search coordinates gave a model having a structure factor residual of 0.506. Six cycles of rigid body refinement (resolution 4–8 Å), still within Merlot, reduced the residual to 0.437.

Least-squares refinement of the native protein

The program X-PLOR (Brunger, 1990) was used for refinement.[1] Only positional refinement in X-PLOR was

[1] The copper force field used in the program was defined by Dr. Neena Summers, Monsanto Corporation, who verified the parameters with seven type I copper proteins retrieved from the Brookhaven Protein Data Bank. The force field maintained the ligation state of the metal, in the test structures, during energy minimization and simulated annealing without significantly altering the resulting geometry. The parameters will be included in future releases of X-PLOR.

Table 7. *Molecular replacement results of amicyanin*

Program	Peak rank	% Maximum[a] or R-factor[b]	Relative σ[c]	α	β	γ	X[d]	Y[d]	Z[d]
CROSUM[e]	1	100.00	8.5	57.5	42.0	185.0	–	–	–
	2	96.52	4.2	75.0	62.0	160.0	–	–	–
TRNSUM[f]	1	100.0	6.1	–	–	–	0.46	0.50	0.38
	2	47.0	2.8	–	–	–	0.18	0.50	0.34
RMINIM[g]	–	0.437	–	57.57	41.93	184.23	0.460	0.000	0.383

[a] Percentage of the maximum peak height in the program CROSUM.
[b] R-factor found by program RMINIM.
[c] Ratio of peak height to the root mean square value of the rotation function.
[d] X, Y, and Z are the fractional coordinates of the search model in the amicyanin cell.
[e] Crowther rotation function. The increments in α, β, and γ were 2.5°, 2°, and 5°, respectively.
[f] Crowther-Blow translation function (Crowther & Blow, 1967).
[g] Rigid body R-factor minimization program (Fitzgerald, 1988).

used for the analysis, which is equivalent to the conventional restrained least-squares procedure (Hendrickson & Konnert, 1980). The initial refinement was done for the native protein at 3–8 Å resolution with all B-factors fixed at 15 Å^2. After 160 steps of positional refinement the R-factor had dropped from 44.9% to 26.3%. The $F_o - F_c$ and $2F_o - F_c$ difference maps were examined and a loop consisting of residues 17–21 and the side chain of residue 31 were adjusted. After 40 more cycles of positional refinement this model gave an R-factor of 25.1%. The refinement was extended to 2.0 Å resolution in several stages and included refinement of individual atomic temperature factors in the later stages. At this point the R-factor was 26.1% for data between 2.0 and 8.0 Å. The model was again compared to its $F_o - F_c$ and $2F_o - F_c$ maps, several regions were readjusted, and the model was refined to a residual R-factor of 23.9%. At this point solvent molecules were introduced to the model. Peaks on the $F_o - F_c$ map above a 4σ contour level were examined for their chemical suitability as the oxygens of water molecules. If the peak shape and interatomic contacts were reasonable, the peak was modeled as a water molecule. At this stage the peaks close to the 17–21 loop region were not included, as this loop still showed broken density in the $2F_o - F_c$ map at 1σ contour level. Peaks close to the N- or C-terminal regions also were not modelled as solvent until the R-factor fell below 18%. A total of 89 water molecules were added after minor remodelling. A total of 5,910 reflections between 2.0 and 8.0 Å resolution were used to refine the positions and temperature factors of 897 atoms. The final R-factor was 15.7% with rms deviations from ideal bond lengths and angles of 0.014 Å and 2.9°, respectively.

Refinement of apoamicyanin

Because amicyanin and apoamicyanin are isomorphous, the copper atom could be removed from the amicyanin model and the polypeptide coordinates refined directly with the apoamicyanin data. The model of amicyanin that was used to initiate refinement was one that had been refined to 2.0 Å but had undergone only minimal refitting and only one cycle of temperature factor refinement. Positional refinement at a resolution of 3.0–8.0 Å reduced the R-factor from an initial value of 22.9% to 18.3%. The resolution was gradually extended to 1.8 Å, the limit of data collection, by restrained positional and temperature factor refinement, but with no manual refitting. Before the addition of any waters the R-factor was 23.1% for the data between 1.8 and 8 Å. After minor readjustment of the model and the addition of 95 water molecules, a final R-factor of 15.5% was achieved using 8,221 reflections between 1.8 and 8 Å resolution. The total number of atoms included in the final refinement was 905. The deviations from ideal bond lengths and angles were 0.011 Å and 2.8°, respectively.

Acknowledgments

We thank Dr. Neena Summers for providing us with the parameters for the copper ion that were used in X-PLOR. This work was supported by NSF grant MCB-9119789 and USPHS grant GM41574.

References

Adman, E.T. (1985). Structure and function of small blue copper proteins. In *Metalloproteins*, Vol. 1 (Harrison, P.M., Ed.), pp. 1–42. Verlag Chemie, Berlin.

Adman, E.T., Turley, S., Bramson, R., Petratos, K., Banner, D., Tsernoglou, D., Beppu, T., & Watanabe, H. (1989). A 2.0 Å structure of the blue copper protein (cupredoxin) from *Alcaligenes faecalis* S-6. *J. Biol. Chem. 264*, 87–99.

Ambler, R.P. & Tobari, J. (1985). The primary structures of *Pseudomonas* AM1 amicyanin and pseudoazurin. *Biochem. J. 232*, 451–457.

Baker, E.N. (1988). Structure of azurin from *Alcaligenes denitrificans*. Refinement at 1.8 Å resolution and comparison of the two crystallographically independent molecules. *J. Mol. Biol. 203*, 1071–1095.

Brunger, A.T. (1990). *XPLOR Manual, v. 2.1.* Yale University, New Haven, Connecticut.

Chapman, S.K. (1991). Blue copper proteins. In *Perspectives on Bioinorganic Chemistry*, Vol. 1 (Hay, R.W., Dilworth, J.R., & Nolan, K.B., Eds.), pp. 95–140. JAI Press Ltd., London.

Chen, L., Durley, R., Poliks, B.J., Hamada, K., Chen, Z., Mathews, F.S., Davidson, V.L., Satow, Y., Huizinga, E., Vellieux, M.D., & Hol, W.G.J. (1992). Crystal structure of an electron transfer complex between methylamine dehydrogenase and amicyanin. *Biochemistry 31*, 4959–4964.

Chen, L., Lim, L.W., Mathews, F.S., Davidson, V.L., & Husain, M. (1988). Preliminary X-ray crystallographic studies of methylamine dehydrogenase and methylamine dehydrogenase–amicyanin complexes from *Paracoccus denitrificans*. *J. Mol. Biol. 203*, 1137–1138.

Chou, P.Y. & Fasman, G.D. (1977). β-Turns in proteins. *J. Mol. Biol. 115*, 135–175.

Collyer, C.A., Guss, J.M., Sugimura, Y., Yoshizaki, F., & Freeman, H.C. (1990). Crystal structure of plastocyanin from a green alga, *Enteromorpha prolifera*. *J. Mol. Biol. 211*, 617–632.

Crawford, J.L., Lipscomb, W.N., & Schellman, C.G. (1973). The reverse turn as a polypeptide conformation in globular proteins. *Proc. Natl. Acad. Sci. USA 70*, 538–547.

Crowther, R.A. & Blow, D.M. (1967). A method of positioning a known molecule in an unknown crystal structure. *Acta Crystallogr. 23*, 544–548.

Fitzgerald, P.M.D. (1988). MERLOT, an integrated package of computer programs for the determination of crystal structures by molecular replacement. *J. Appl. Crystallogr. 21*, 273–278.

Garrett, T.P.J., Clingeleffer, D.J., Guss, J.M., Rogers, S.J., & Freeman, H.C. (1984). The crystal structure of poplar apoplastocyanin at 1.8 Å resolution. *J. Biol. Chem. 259*, 2822–2825.

Godden, J.W., Turley, S., Teller, D.C., Adman, E.T., Yiu, M.Y., Payne, W.J., & LeGall, J. (1991). The 2.3 Å X-ray structure of nitrite reductase from *Achromobacter cycoclastes*. *Science 253*, 438–442.

Gray, K.A., Davidson, V.L., & Knaff, D.B. (1988). Complex formation between methylamine dehydrogenase and amicyanin from *Paracoccus denitrificans*. *J. Biol. Chem. 263*, 13987–13990.

Guss, J.M. & Freeman, H.C. (1983). Structure of oxidised plastocyanin at 1.6 Å resolution. *J. Mol. Biol. 169*, 521–563.

Guss, J.M., Harrowell, P.R., Murata, M., Norris, V.A., & Freeman, H.C. (1986). Crystal structure analyses of reduced (Cu^{I}) poplar plastocyanin at six pH values. *J. Mol. Biol. 192*, 361–387.

Guss, J.M., Merritt, E.A., Phizackerley, R.P., Hedman, B., Murata, M., Hodgson, K.O., & Freeman, H.C. (1988). Phase determination by multiple-wavelength X-ray diffraction: Crystal structure of a basic "blue" copper protein from cucumbers. *Science 241*, 806–811.

He, S., Modi, S., Bendall, D.S., & Gray, J.C. (1991). The surface exposed tyrosine residue Tyr83 of pea plastocyanin is involved in both binding and electron transfer reactions with cytochrome f. *EMBO J. 10*(13), 4011–4016.

Hendrickson, W.A. & Konnert, J.H. (1980). Stereochemically restrained crystallographic least squares refinement of macromolecular structures. In *Biomolecular Structure, Function, Conformation and Evolution*, Vol. 1 (Srinivasan, R., Ed.), pp. 43–57. Pergamon, Oxford, UK.

Husain, M. & Davidson, V.L. (1985). An inducible periplasmic blue copper protein from *Paracoccus denitrificans*. *J. Biol. Chem. 260*, 14626–14629.

Husain, M., Davidson, V.L., & Smith, A.J. (1986). Properties of *Paracoccus denitrificans*. *Biochemistry 25*, 2431–2436.

Kabsch, W. & Sander, C. (1983). Dictionary of protein secondary structure: Pattern recognition of hydrogen-bonded and geometric features. *Biopolymers 22*, 2577–2637.

Lim, L.W., Mathews, F.S., Husain, M., & Davidson, V.L. (1986). Preliminary X-ray crystallographic study of amicyanin from *Paracoccus denitrificans*. *J. Mol. Biol. 189*, 257–258.

Lim, L.W., Mathews, F.S., & Steenkamp, D.J. (1982). Crystallographic study of the iron-sulphur flavoprotein trimethylamine dehydrogenase from the bacterium W_3A_1. *J. Mol. Biol. 162*, 869–876.

Lommen, A. & Canters, G.W. (1990). pH-dependent redox activity and fluxionality of the copper site in amicyanin from *Thiobacillus versutus* as studied by 300- and 600-MHz ^{1}H NMR. *J. Biol. Chem. 265*, 2768–2774.

Lommen, A., Pandya, K.I., Koningsberger, D.C., & Canters, G.W. (1991a). EXAFS analysis of the pH dependence of the blue-copper site in amicyanin from *Thiobacillus versutus*. *Biochim. Biophys. Acta 1076*, 439–447.

Lommen, A., Wijmenga, S., Hilbers, C.W., & Canters, G.W. (1991b). Assignment of the 600 MHz ^{1}H-NMR spectrum of amicyanin from *Thiobacillus versutus* by 2D-NMR methods provides for information on secondary structure. *Eur. J. Biochem. 201*, 695–702.

Matthews, B.W. & Czerwinski, E.W. (1975). Local scaling: A method to reduce systematic errors in isomorphous replacement and anomolous scattering measurement. *Acta Crystallogr. A31*, 480–487.

Messerschmidt, A., Ladenstein, R., Huber, R., Bolognesi, M., Avigiliano, L., Petruzzelli, R., Rossi, A., & Finazzi-Agro, A. (1992). Refined crystal structure of ascorbate oxidase at 1.9 Å resolution. *J. Mol. Biol. 224*, 179–205.

Nar, H., Messerschmidt, A., Huber, R., van de Kamp, M., & Canters, G. (1991). Crystal structure analysis of oxidized *Pseudomonas aeruginosa* azurin at pH 5.5 and pH 9.0. *J. Mol. Biol. 221*, 765–772.

Nar, H., Messerschmidt, A., Huber, R., van de Kamp, M., & Canters, G.W. (1992). Crystal structure of *Pseudomonas aeruginosa* apoazurin at 1.85 Å resolution. *FEBS Lett. 306*, 119–124.

Petratos, K., Dauter, Z., & Wilson, K.S. (1988). Refinement of the structure of pseudoazurin from *Alcaligenes faecalis* S-6 at 1.55 Å resolution. *Acta Crystallogr. B44*, 628–636.

Ramachandran, G.N. & Sasisekharan, V. (1968). Conformation of polypeptides and proteins. *Adv. Protein Chem. 23*, 283–437.

Ryden, L. (1984). Structure and evolution of the small blue protein. In *Copper Proteins and Copper Enzymes*, Vol. 1 (Lontie, R., Ed.), pp. 157–182. CRC Press, Boca Raton.

Sharma, K.D., Loehr, T.M., Sanders-Loehr, J., Husain, M., & Davidson, V.L. (1988). Resonance raman spectroscopy of amicyanin, a blue copper protein from *Paracoccus denitrificans*. *J. Biol. Chem. 263*, 3303–3306.

Tobari, J. & Harada, Y. (1981). Amicyanin: An electron acceptor of methylamine dehydrogenase. *Biochem. Biophys. Res. Commun. 101*, 502–508.

van Beeumen, J., van Bun, S., Canters, G.W., Lommen, A., & Chothis, C. (1991). The structural homology of amicyanin from *Thiobacillus versutus* to plant plastocyanins. *J. Biol. Chem. 266*, 4869–4877.

van de Kamp, M., Silvestrini, M.C., Brunori, M., van Beeumen, J., Hali, F.C., & Canters, G.W. (1991). Involvement of the hydrophobic patch of azurin in the electron-transfer reactions with cytochrome c_{551} and nitrite reductase. *Eur. J. Biochem. 194*, 109–118.

van Spanning, R.M.J., Wansell, C.W., Reijnders, W.N.M., Oltmann, L.F., & Stouthamer, A.H. (1990). Mutagenesis of the gene encoding amicyanin of *Paracoccus denitrificans* and the resultant effect on methylamine oxidation. *FEBS Lett. 275*, 217–220.

Venkatachalam, C.M. (1968). Stereochemical criteria for polypeptides and proteins. *Biopolymers 6*, 1425–1436.